

Supporting Information

Complete amplitude and phase control of light using broadband holographic metasurfaces

Gun-Yeal Lee,^a Gwanho Yoon,^b Seung-Yeol Lee,^c Hansik Yun,^a Jaebum Cho,^a Kyoookun Lee,^a

*Hwi Kim,^d Junsuk Rho,^{a, e} & ByoungHo Lee^{*a}*

^aSchool of Electrical and Computer Engineering and Inter-University Semiconductor Research Center, Seoul National University, Gwanak-Gu Gwanakro 1, Seoul 08826, Republic of Korea

^bDepartment of Mechanical Engineering, Pohang University of Science and Technology (POSTECH), Pohang 37673, Republic of Korea

^cSchool of Electronics Engineering, College of IT Engineering, Kyungpook National University, buk-gu daehakro 80, Daegu 702-701, Republic of Korea

^dDepartment of Electronics and Information Engineering, Korea University, 2511 Sejong-ro, Sejong 339-700, Republic of Korea

^eDepartment of Chemical Engineering, Pohang University of Science and Technology (POSTECH), Pohang 37673, Republic of Korea

*corresponding author email: byoungHo@snu.ac.kr

Part 1. A reflection-type X-shaped meta-atom

Although we discuss the transmission-type metasurfaces in the main text, the concept of X-shaped meta-atoms can be applied to implement a reflective metasurface. In this section, the optimized design of the reflective metasurface with X-shaped meta-atoms is introduced. To increase the efficiency of modulation by metasurfaces, a multi-layered structure such as a metal-dielectric-metal waveguide was proposed as reflection type.¹ By the reference [1], the authors well designed their multi-layered structures using a geometric phase and got high efficiency for broadband wavelengths in near-infrared region. However, same structure is hard to be applied on visible light such as green and blue light with short wavelengths due to increased optical loss properties of metal. To overcome the drawbacks of low efficiency, we design a modified structure, where metal scatterers are replaced by dielectric material ones. We also choose Poly-Si as a dielectric material due to high refractive index and low loss in visible light. Therefore, the metasurfaces that have Poly-Si/MgF₂/gold layered structure are designed as shown in Fig. 2. In the proposed structure, MgF₂ and gold are used as a spacer and reflecting mirror for Fabry–Pérot resonance, respectively. The geometric parameters such as the geometrics of X-shaped meta-atoms and thicknesses of stacks are optimized in consideration of feasibility and efficient modulation. The thickness of Poly-Si (t_{Si}) and spacer (t_{gap}) are set to 128 nm and 130 nm, respectively. The length of nanorod (L) is 280 nm whereas the width of nanorod (w) is 65 nm. The proposed structure is designed to operate on the mid-visible light with the wavelength of 532 nm. The period of unit-cells is set as 350 nm which is shorter than the wavelength of light at both air and spacer, which means there are no diffraction orders in both sides.

To verify the performances of structures, commercial software (COMSOL Multiphysics 5.0) based on the finite element method (FEM) was used. In the simulation, periodic boundary

conditions were used with the period of 350 nm, and the refractive indices of the materials are based on the reference.² We calculate the S-parameters which are defined as the ratio of complex-amplitude of reflected and modulated light to incident light. Figure 3 shows the cross-polarized component of reflected light as the change of orientation angles (θ_1) and angular disparity (α) on the complex domain. The left figure is the result of theoretical calculation where the X-shaped meta-atom is assumed as double electric dipoles whose directions are parallel to the arms of the X-shaped structure. On the other hand, the right figure is corresponding results of the FEM simulation for the actual X-shaped structure. As a result, in the Fig. 3, the maximum efficiency, which is defined as efficiency for maximum amplitude condition, almost reaches 40% at the wavelength of 532 nm. As shown in Fig. 3, both theoretical and simulation results have almost the same tendency, and entire ranges of the complex domain are fully covered. The difference of two orientation angles is related with the amplitude of S-parameters, whereas the sum of two orientation angles is related with the phase of S-parameters. Therefore, we can confirm that X-shaped meta-atoms can be implemented in both transmission- and reflection-type metasurfaces.

Part 2. Numerical simulation

The results in Figs. 1d and 2 were performed by commercial software (COMSOL Multiphysics 5.0) based on the finite element method (FEM). In the simulation, the periodic boundary conditions were used with the period of 350 nm. The material indices constructing the structures are based on the reference.⁵⁰ In Fig. 1d, electric fields with polarization vectors are calculated on the xy-plane at the upper surface of the X-shaped meta-atom. For Fig. 2, The transmission coefficients of the proper polarizations are computed for all combined values of the orientation angles θ and the angular disparity α in the range from 0° to 180° and from 60° to 90° , respectively. The period of the unit cell is set to 350 nm. The simulation results in Figs. 4d and 4e for holographic images were calculated by using Fresnel diffraction theory. For these simulations, the input light is assumed as an ideal plane wave with normal incidence. Desired phase and amplitude profiles represented in the upper side of Fig. 4d are then multiplied to the plane wave, and the z-directional propagations of them are calculated for proper image planes by using the angular spectrum methods.³

Part 3. Device fabrication

Standard electron-beam lithography processes with lift-off and etching processes were used to fabricate the metasurfaces. First, an intrinsic poly-crystalline silicon (Poly-Si) film with 128 nm thickness was deposited on a fused silica wafer using low-pressure chemical vapor deposition (Eugene Technology BJM-100) at the temperature of 700°C . Then, an electron-beam lithography (Elionix ELS-7800) and a standard lift-off process were used to create the designed X-shaped patterns with chromium (Cr) hard-mask layer. Inductive coupled plasma based reactive ion

etching (ULVAC NE-7800) was employed to etch the Poly-Si layer along the patterned Cr, and Cr masks were then removed by using chromium etchant (KMG CR-7) after all of the processes.

Part 4. Optical measurement

A schematic of the optical set-up is depicted in Fig. S1. A high-power optically pumped semiconductor laser (OPSL; Coherent, Verdi G2 SLM) with a wavelength of 532 nm illuminates the back side of the metasurfaces after passing through a spatial filter, a half-wave plate (HWP), a quarter-wave plate (QWP), and an iris. To generate well-collimated beams, a beam spatial filter was used to eliminate the high orders of the Gaussian beam. The HWP and QWP were employed to set the polarization of incident beam into the right circular polarization state, and the iris was for restricting multiple reflections among the optic elements. A visible polarimeter (Thorlabs, PAN5710VIS) was used to precisely generate the proper polarization state. The metasurfaces samples and the lens are mounted on XYZ stages to carefully steer the relative positions on the beam path. In the measurements, the beam radius was set to be about 500 μm , which is fully larger than the size of metasurfaces ($\sim 210 \mu\text{m}$). The optical microscopy, which consists of the objective lens and the tube lens, was applied to measure the images at proper image planes, and the visible charge-coupled device (CCD) camera captured images. To measure the results in Fig. 5, the laser in the schematic of Fig. S1 was exchanged to other optical lasers of which wavelengths are 660 nm (Cobolt, Flamenco 300) and 473 nm (Spectra-Physics, Excelsior 473) for red and blue colours, respectively. To obtain the maximum efficiencies of the metasurfaces, the same optical setup in Fig. S1 is used except the CCD camera, which is exchanged to the set of pinhole and a power meter device. The optical power passed through the metasurface and the pinhole was measured using the power meter and divided by the power of the incident beam.

Part 5. Design of Holograms

The angular spectrum method (ASM) was used to calculate computer generated holograms (CGHs). The ASM is a method based on the diffraction optics to calculate diffracted light fields by decomposing light field into plane waves. In the process of ASM, there is no paraxial approximation, so it is appropriate to calculate holograms with wide bandwidth. Target images consist of three letters of “SNU”, of which each alphabet is at different depth planes. To calculate, each letter image at the different depth is back-propagated to the metasurface plane by ASM. By integrating all back-propagated profiles on the metasurface plane, finally, the CGH can be well calculated because ASM is well defined between parallel planes. Here, continuous and full ranges of amplitude and phase were used to construct the CGH without any discrete levels, which makes more clear holographic images. Due to the advantage of full complex-amplitude modulation capability, CGH is calculated without any support of optimization algorithms such as the Gerchberg-Saxton (GS) algorithm. The phase-only CGH in the upper side of Fig. 4e was also calculated for the comparison with the full complex CGH. The phase-only CGH was calculated from the complex CGH by flattening its amplitude profiles. For the fair comparison, additional optimization algorithms such as the GS algorithm were not applied to the phase-only CGH. The GS algorithm can improve an accuracy of amplitude profiles on the image plane. However, this algorithm causes that the phase profile on the image plane, which should be a degree of freedom, cannot be controlled as desired. It is worth noting that this is the critical limitation of GS algorithm for practical three-dimensional holograms. A target wavelength is set to 532 nm, and the sampling period of the CGH is set to 350 nm. All the fabricated devices in this research have identical pixel numbers (600×600 pixels).

SUPPLEMENTARY FIGURES

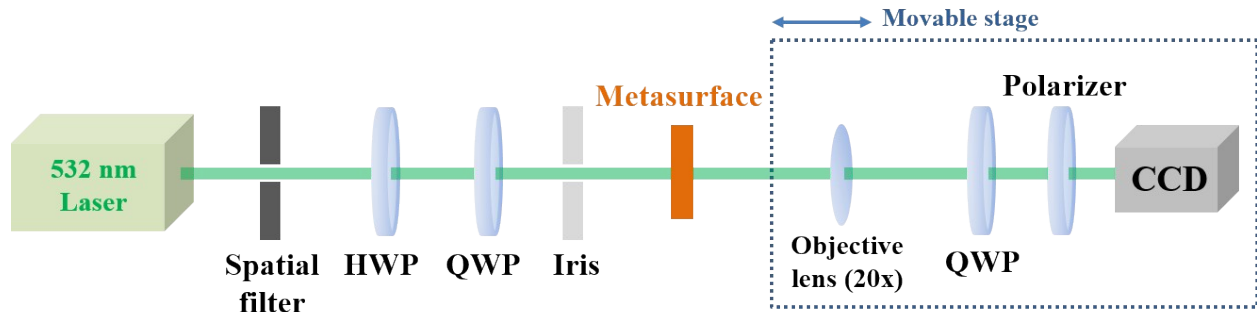


Figure S1. Measurement setup with an optical microscopy. The illustration shows the entire optical set-up for measurements. A laser with wavelength of 532 nm (Coherent, Verdi G2 SLM) generate a light beam, which illuminates back side of metasurfaces after penetrating the optical elements including a spatial filter, a half-wave plate, a quarter-wave plate, and an iris. An objective lens with magnitude of 20 and coupled-charge device (CCD) camera are used to measure the transmitted light from the metasurfaces, and cross-polarized analyzer with a QWP and a polarizer was used to filter the cross-polarized component of the transmitted light. Elements in blue-dotted box are on a movable stage to measure different focal planes.

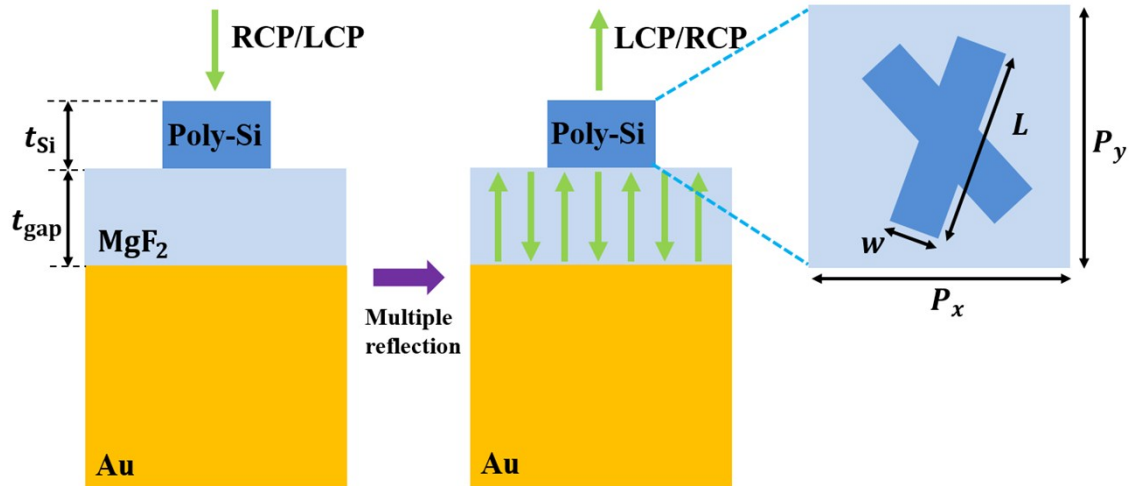


Figure S2. Schematic cross-section of reflective metasurfaces. The pixels are arranged with $P_x = P_y = 350$ nm and the thickness of Poly-Si (t_{Si}) and MgF_2 film (t_{gap}) are 128 nm and 130 nm, respectively. The length of nanorod (L) is 280 nm and the shorter length of nanorod (w) is 65 nm. When the circular polarized light normally illuminates to the structure, the MgF_2 film and gold film act as a Fabry–Pérot cavity. The resonance generates the cross-polarized reflected beams with designed amplitude and phase which can be adjusted by orientation angles and angular disparities of X-shaped meta-atoms.

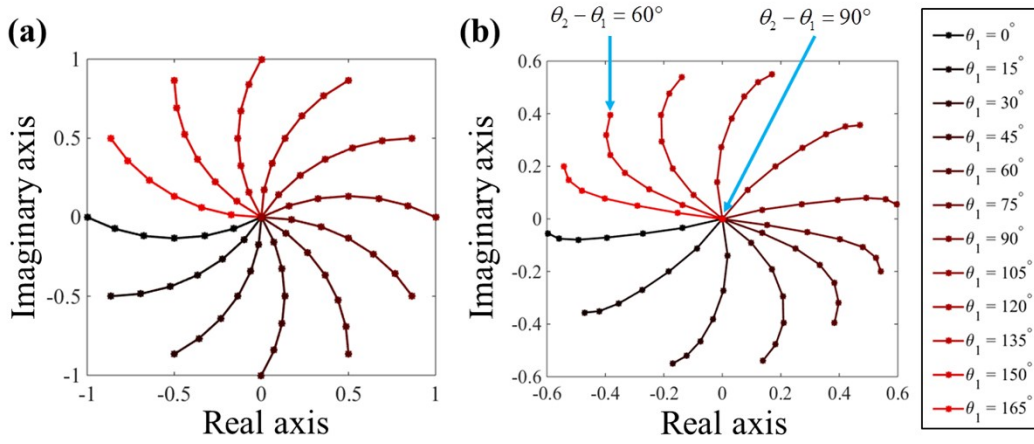


Figure S3. Calculated cross-polarized reflection coefficients. Results of measured cross-polarized reflection coefficients represented on the complex domain based on (a) theoretical calculation and (b) FEM simulation. Each line with distinct color has different orientation angle θ_1 , and points in the same color line have different angular disparity α . The angular disparity α is 90° at the center of graph and decreases when the points become away from the center of graph. At the edge of the graph, the angular disparity becomes 60° , which is the smallest.

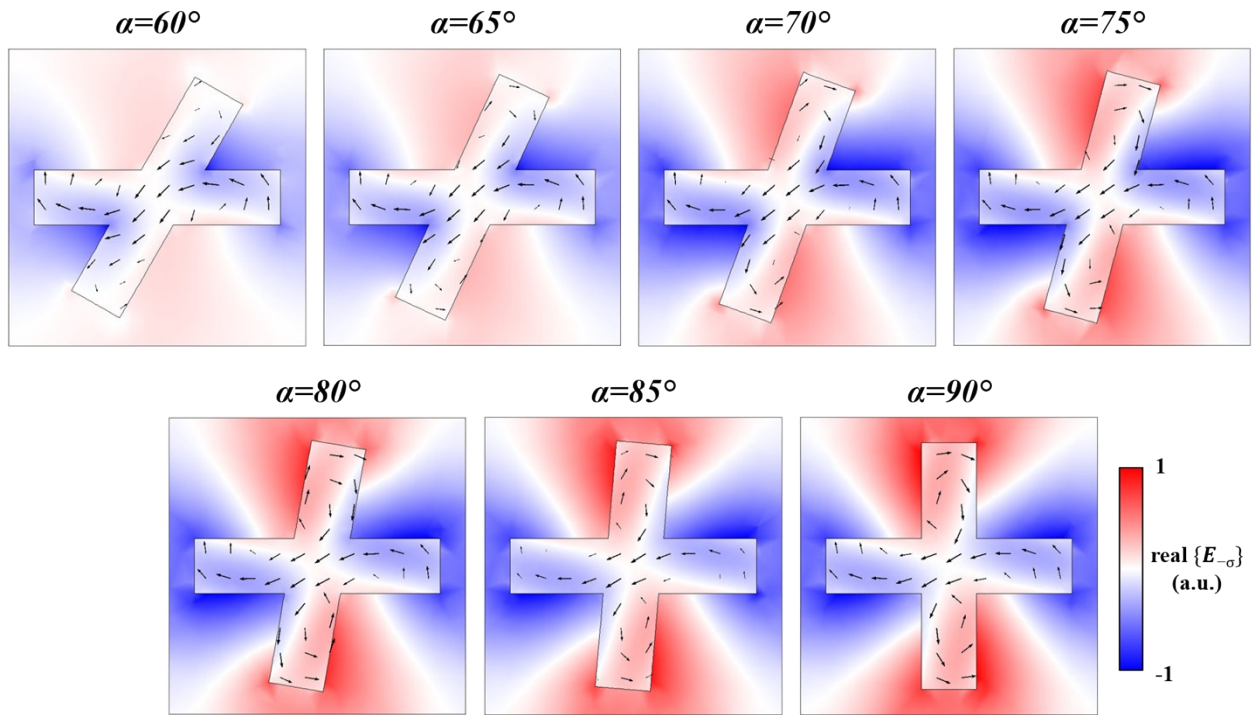


Figure S4. Two dimensional maps with electric fields and polarization vectors from FEM simulations. X-shaped meta-atoms with angular disparities from $\alpha = 60^\circ$ to $\alpha = 90^\circ$ are calculated by FEM simulations. In the figures, colors represent the real part of cross-polarized electric fields ($E_{-\sigma}$), and black arrows in the figures represent the magnitudes and directions of the polarization vectors at each position. The boundary of the figures means the unit-cell boundary of which period is 350 nm.

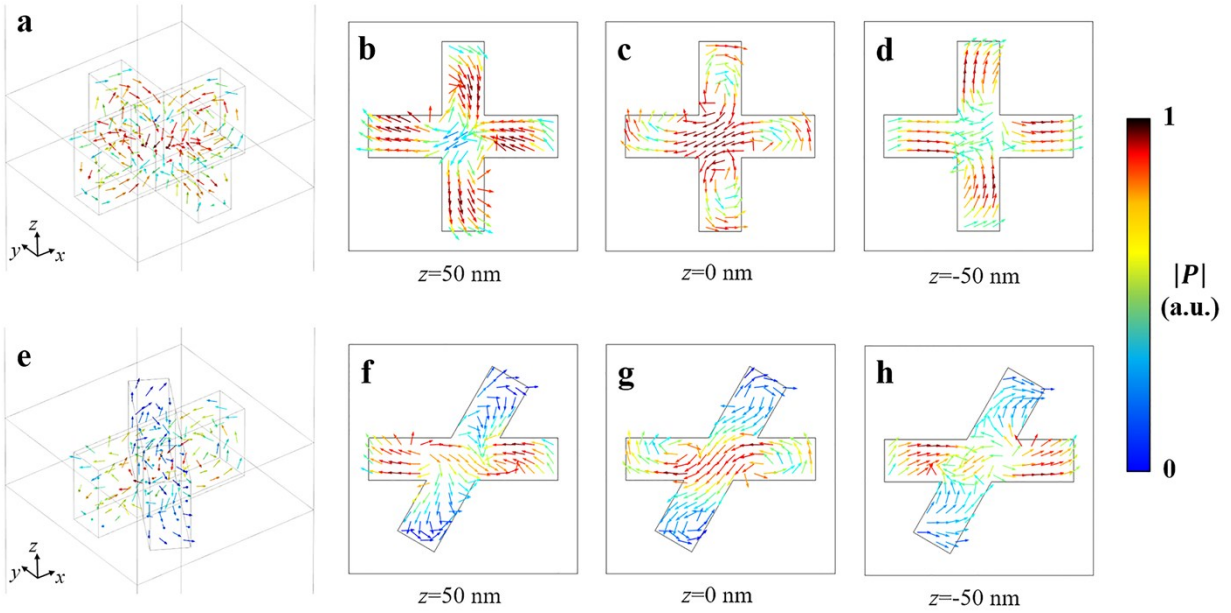


Figure S5. Polarization vector distributions for the X-shaped meta-atom with (a–d) $\alpha = 60^\circ$ and (e–h) $\alpha = 90^\circ$ under right circularly polarized incidence. (a, e) Polarization vector distributions in three-dimensional domain where the direction of arrows represents the direction of the polarization vector and the color of the arrow represents the magnitude of the polarization vector. Polarization vector distributions are represented for several cross sections at the (b, f) top, (c, g) center, and (d, h) bottom of the X-shaped meta-atom, respectively.

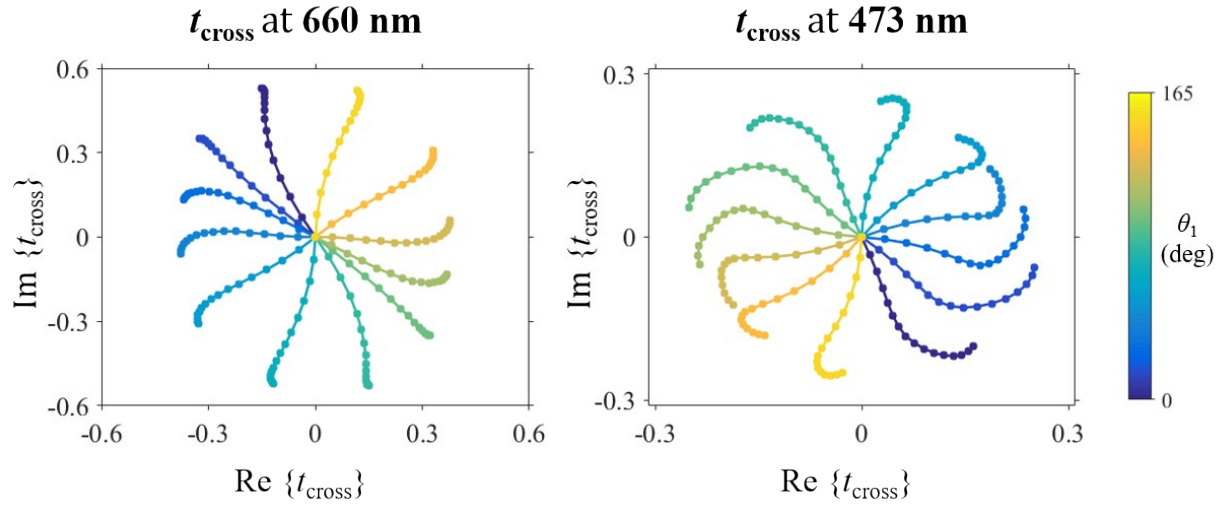


Figure S6. FEM simulation results of cross-polarized transmission coefficient (t_{cross}) for several wavelengths. The wavelengths of 660 nm and 473 nm are considered. Accessible range of t_{cross} plotted in the complex domain. The different colors of the lines represent the cases of different orientation angles, and the color bar is explained on the right side of the graphs. The points in the same line have same orientation angle, but with different angular disparities from $\alpha = 60^\circ$ to $\alpha = 90^\circ$. The point at center is for $\alpha = 90^\circ$ and the point at edge is for $\alpha = 60^\circ$, and the angular disparity decreases when the point becomes far from the center.

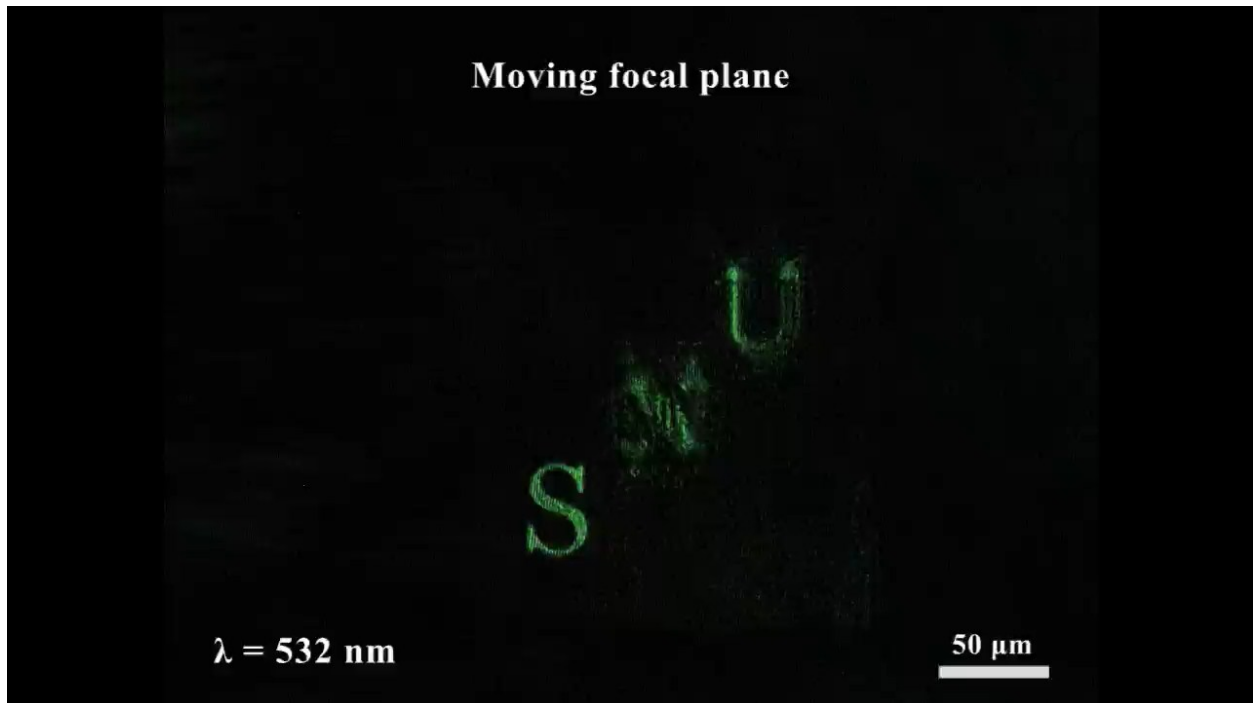


Figure S7. Explanation on Movies S1–S3. Video clips are experimentally recorded for continuous changes of the holographic images with respect to z -position. Movie S1 is corresponding to Fig. 4d in the main article while Movies S2 and S3 are corresponding to Fig. 5. Operating wavelengths λ of 532 nm, 660 nm, and 473 nm are considered in Movies S1, S2, and S3, respectively. In the video, the focal plane is changed from “S” plane to “N” plane, and then “N” to “S”, reversely, where the “U” plane is located between “S” and “N”. This change is repeated twice in the entire play time.

SUPPLEMENTARY REFERENCES

- [1] G. Zheng, H. Muhlenbernd, M. Kenney, G. Li, T. Zentgraf and S. Zhang, *Nat. Nanotech.*, 2015, **10**, 308-312.
- [2] M. J. Weber, *Handbook of Optical Materials*, ed. CRC Press, Boca Raton, 2003.
- [3] J. W. Goodman, *Introduction to Fourier Optics*, ed. Robert & Company Publisher, Englewood, 2005.